A Unified Approach for LRFD Live Load Moments in Bridge Decks

by

Christopher Higgins[1], O. Tugrul Turan[2], Robert J. Connor[3], and Judy Liu[3]

Abstract

Current AASHTO-LRFD specifications use many disparate design provisions to establish live load demands in bridge decks. As an example, approximately 17% of Chapter 4 addresses analysis of decks. One of the AASHTO-LRFD analysis methods for decks uses an orthotropic plate model. The present AASHTO-LRFD orthotropic plate model has a single formulation for the plate torsional stiffness and this is not generally applicable to all deck types. In this paper, new analytical expressions are developed for moment in bridge decks subjected to arbitrary patch loading considering each of the three cases of orthotropy: 1) relatively torsionally stiff, flexurally soft decks; 2) relatively uniformly thick deck (such as a reinforced concrete deck); and 3) relatively torsionally soft, flexurally stiff decks. Using these newly developed expressions, the AASHTO-LRFD notional live load models were combined with impact, multiple presence, and live load factors to determine maximum strong direction live load moments for the Strength I design limit state. Design equations were developed to estimate the maximum strong direction live load moments without having to perform cumbersome moving load analysis for common deck orientations. Using the proposed formulations, bridge deck strength design demands can now be treated in a unified way across different deck types using only four equations. Application of these methods can significantly reduce and

[1] Professor and Slayden Construction Faculty Fellow, [2] Post-Doctoral Research Associate, School of Civil and Const. Engineering, Oregon State University, Corvallis, OR 97331
[3] Assoc. Professor, School of Civil Engineering, Purdue University, West Lafayette, IN 47907

simplify the analysis of decks and allow bridge engineers to make comparisons across different deck design alternatives.

Introduction and Background

Many different types of bridge decks are deployed for both new design and rehabilitation of existing bridges. These decks include cast-in-place reinforced concrete; open grid; steel grid deck systems fully or partially filled with concrete; as well as open and closed-ribbed composite, concrete, aluminum, and steel systems. Presently, analysis of decks is principally treated in the AASHTO-LRFD Specifications (2007) in Chapter 4. Over 17% of Chapter 4 is spent addressing deck analysis with methods that range from historical practice to sophisticated modern treatments. The methods vary in the differing modeling assumptions, load placement requirements, and analysis simplifications. As a result, designers cannot make direct comparisons between possible alternatives and the design provisions do not elucidate the characteristics that ***would allow an engineer to understand the role of the deck stiffness components on deck flexural behavior and load distribution in any deep and meaningful way***. This current situation calls for a unified analytical approach, based on engineering mechanics, to establish design live load moments across all bridge deck types. Such an approach is developed and proposed here.

Because of the different size, spacing, and distribution of the components that make up a deck, bridge decks can generally be considered orthotropic structures, exhibiting different elastic stiffness properties in two orthogonal directions. For cases where the stiffnesses are similar in the orthogonal directions, the resulting isotropic response is merely a special case of orthotropy. Even for those deck systems designed for parallel longitudinal stringers, the orthotropic nature of a deck can strongly influence the structural behavior (such as moment magnitude under tire patch loading). Although most deck systems are geometrically orthotropic, they have generally been treated as materially orthotropic and analyzed utilizing orthotropic thin plate theory. Baker (1991), (concrete filled steel grid system (CFSGS)); Gangarao *et al.* (1992), (CFSGS); Mangelsdorf *et al.* (2002), (CFSGS); Huang *et al.* (2002) (open steel grid deck (OSGD)); Higgins (2003, 2004), (CFSGS); and Huang *et al.* (2007) (CFGS) have all used orthotropic thin plate theory for analyzing bridge decks.

The present American Association of State Highway Officials Load and Resistance Factor Design Specification (AASHTO-LRFD, 2007) accepts orthotropic plate analysis as a permissible technique and section 4.6.2.1.8 includes design moment demands for fully and partially filled grids and unfilled grid decks composite with reinforced concrete slabs that are based on an orthotropic plate formulation. These design equations envelope the load effects produced from the specified notional load combinations such as the design tandem and multiple truck tire patches (Higgins, 2003). The orthotropic plate model can be reduced to isotropic by setting the stiffness ratio between the strong and weak directions to unity and thus design demands in section 4.6.2.1.8 can be compared with those prescribed in AASHTO-LRFD Table A4-1. As seen in Fig. 1, the design demand moments from the orthotropic plate model (reduced to isotropic by setting D=1.0) correspond reasonably well to those specified for traditional design of concrete decks. It is important to note that the original AASHTO-LRFD orthotropic plate model formulation in section 4.6.2.1.8 was not calibrated to these traditional moments and yet the outcomes are reasonably coincident for the common transverse to traffic case. This further indicates that a unified analysis theory based on general orthotropic plate theory may provide consistency in design demands across different deck types.

The original semi-analytical solutions (Higgins 2003) were derived for a particular case of torsional stiffness which is typically representative of a uniformly thick deck. Thus these equations are not generally applicable to systems with differing relative torsional stiffnesses that would be of practical consideration (for example closed-ribbed, sandwich, or open grid decks). Recently, an analytical study developed deflection equations for orthotropic plates subjected to arbitrary patch loading that include all three cases of orthotropy: 1) relatively torsionally stiff, flexurally soft decks; 2) relatively uniformly thick decks (reinforced concrete deck); and 3) relatively torsionally soft, flexurally stiff decks (Turan, 2009). Utilizing these equations, this paper develops Strength I design live load moment equations considering factored load combinations including the design tandem and multiple truck tire patches that enables bridge decks to be considered in a unified way in the AASHTO-LRFD Specification. By treating all decks in a uniform and consistent manner, implementation of the design equations in the AASHTO-LRFD Specification would dramatically simplify analysis of bridge decks, while preserving the key structural stiffness parameters that elucidate load distribution characteristics and thus allow designers to better assess design alternatives.

Orthotropic Plate Theory

The general differential equation for bending and twisting moments of an orthotropic thin plate can be written as (Timoshenko and Woinowski-Krieger, 1959):

$$D_x \frac{\partial^4 w}{\partial x^4} + 2H \frac{\partial^4 w}{\partial x^2 \partial y^2} + D_y \frac{\partial^4 w}{\partial y^4} = q(x, y) \text{ ; } H = D_1 + 2D_{xy} \tag{1}$$

$$M_x = -(D_x \frac{\partial^2 w}{\partial x^2} + D_1 \frac{\partial^2 w}{\partial y^2}) \tag{2}$$

$$M_y = -(D_y \frac{\partial^2 w}{\partial y^2} + D_1 \frac{\partial^2 w}{\partial x^2}) \tag{3}$$

$$M_{xy} = 2D_{xy} \frac{\partial^2 w}{\partial x \partial y} \tag{4}$$

where D_x is the flexural rigidity in the strong direction, D_y is the flexural rigidity in the weak direction, D_1 is the torsional rigidity contribution from the strong and the weak direction rigidities, D_{xy} is the torsional rigidity, H is the sum of the torsional rigidity contribution from the strong and weak direction rigidities (D_1) and torsional rigidity (D_{xy}), $w(x, y)$ is the vertical plate deflection in the Cartesian coordinate system, and $q(x, y)$ is the applied transverse load in the Cartesian coordinate system, respectively.

Depending on the torsional rigidity of the plate, there are 3 possibilities (Timoshenko and Woinowski-Krieger, 1959):

Case 1. $H > \sqrt{D_x D_y}$; the solution has real and unequal roots which corresponds to relatively torsionally stiff, flexurally soft decks which correspond to partially and fully filled grid decks.

Case 2. $H = \sqrt{D_x D_y}$; the solution has equal and real roots which corresponds to relatively uniformly thick plate or typical reinforced concrete slab.

Case 3. $H < \sqrt{D_x D_y}$; the solution has imaginary roots which corresponds to relatively torsionally soft, flexurally stiff decks which correspond to open steel grid deck.

Bridge decks can generally be modeled as simply supported infinitely wide plates, as the location of transverse supports are relatively wide and continuity effects are accounted for by modification coefficients. For such boundary conditions, semi-analytical expressions (technically not closed-form due to infinite series) can be developed for bending moments. For a single patch load located on an infinitely wide and simply supported orthotropic plate, as shown in Fig. 2, the moment equations in the strong direction are (Turan, 2009) :

For Case 1:

$$M_x(y \geq \frac{v}{2}) = \frac{2L^2 q}{\pi^3} \sum_{m=1}^{\infty} \frac{1}{m^3} Sin(\frac{m\pi\zeta}{L}) Sin(\frac{m\pi u}{2L}) Sin(\frac{m\pi x}{L}) \\ \times [\frac{t_1^{\,2}}{t_1^{\,2} - t_2^{\,2}} (e^{\frac{-m\pi t_2(2y-v)}{2L}} - e^{\frac{-m\pi t_2(2y+v)}{2L}}) - \frac{t_2^{\,2}}{t_1^{\,2} - t_2^{\,2}} (e^{\frac{-m\pi t_1(2y-v)}{2L}} - e^{\frac{-m\pi t_1(2y+v)}{2L}})] \tag{5}$$

$$M_x(y = 0) = \frac{4L^2 q}{\pi^3} \sum_{m=1}^{\infty} \frac{1}{m^3} Sin(\frac{m\pi\zeta}{L}) Sin(\frac{m\pi u}{2L}) Sin(\frac{m\pi x}{L}) \\ \times [1 + \frac{t_2^{\,2}}{t_1^{\,2} - t_2^{\,2}} e^{\frac{-m\pi t_1 v}{2L}} - \frac{t_1^{\,2}}{t_1^{\,2} - t_2^{\,2}} e^{\frac{-m\pi t_2 v}{2L}}] \tag{6}$$

where $t_1 = \sqrt{\frac{H}{D_y} + \frac{\sqrt{H^2 - D_x D_y}}{D_y}}$ and $t_2 = \sqrt{\frac{H}{D_y} - \frac{\sqrt{H^2 - D_x D_y}}{D_y}}$

For Case 2:

$$M_x(y \geq \frac{v}{2}) = \frac{Lq}{\lambda\pi^2} \sum_{m=1}^{\infty} \frac{1}{m^2} Sin(\frac{m\pi\zeta}{L}) Sin(\frac{m\pi u}{2L}) Sin(\frac{m\pi x}{L}) \\ \times [(\frac{2L\lambda}{m\pi} + y - \frac{v}{2}) e^{\frac{-m\pi(2y-v)}{2L\lambda}} - (\frac{2L\lambda}{m\pi} + y + \frac{v}{2}) e^{\frac{-m\pi(2y+v)}{2L\lambda}}] \tag{7}$$

$$M_x(y = 0) = \frac{4L^2 q}{\pi^3} \sum_{m=1}^{\infty} \frac{1}{m^3} Sin(\frac{m\pi\zeta}{L}) Sin(\frac{m\pi u}{2L}) Sin(\frac{m\pi x}{L}) \times [1 - (1 + \frac{m\pi v}{4L\lambda}) e^{\frac{-m\pi v}{2L\lambda}}] \tag{8}$$

where $\lambda = \left(\frac{D_y}{D_x} \right)^{0.25}$

For Case 3:

$$M_x(y \geq \frac{v}{2}) = \frac{2L^2 q}{\pi^3} \sum_{m=1}^{\infty} \frac{1}{m^3} Sin(\frac{m\pi\zeta}{L}) Sin(\frac{m\pi u}{2L}) Sin(\frac{m\pi x}{L})$$
$$\times [e^{\frac{-m\pi t_1 (2y-v)}{2L}} \left(Cos(\frac{m\pi t_2 (y - \frac{v}{2})}{L}) + \frac{t_1^{\ 2} - t_2^{\ 2}}{2t_1 t_2} Sin(\frac{m\pi t_2 (y - \frac{v}{2})}{L}) \right) \tag{9}$$
$$- e^{\frac{-m\pi t_1 (2y+v)}{2L}} \left(Cos(\frac{m\pi t_2 (y + \frac{v}{2})}{L}) + \frac{t_1^{\ 2} - t_2^{\ 2}}{2t_1 t_2} Sin(\frac{m\pi t_2 (y + \frac{v}{2})}{L}) \right)]$$

$$M_x(y = 0) = \frac{4L^2 q}{\pi^3} \sum_{m=1}^{\infty} \frac{1}{m^3} Sin(\frac{m\pi\zeta}{L}) Sin(\frac{m\pi u}{2L}) Sin(\frac{m\pi x}{L})$$
$$\times e^{\frac{-m\pi t_1 v}{2L}} \left(1 - \left(Cos(\frac{m\pi t_2 v}{2L}) + \frac{t_1^{\ 2} - t_2^{\ 2}}{2t_1 t_2} Sin(\frac{m\pi t_2 v}{2L}) \right) \right) \tag{10}$$

where $t_1 = \sqrt{\frac{\sqrt{\frac{D_x}{D_y}} + \frac{H}{D_y}}{2}}$ and $t_2 = \sqrt{\frac{\sqrt{\frac{D_x}{D_y}} - \frac{H}{D_y}}{2}}$

Case 2 equations are the same equations provided in Higgins (2003) and in all cases Poisson's ratios in the x and y direction were set to zero, which sets D_1 to zero. Generally Poisson's ratio is measured in uniaxial material tests. As described above, since decks are geometrically orthotropic structures and the neutral axis in two orthogonal directions do not coincide, applying normal force along one axis creates not only normal force at the neutral axis but also a force couple on the other orthogonal axis. Thus, empirically measuring Poisson's ratio is impractical. Mangelsdorf *et al.* (2002) (CFSGS); Huang *et al.* (2002) (OSGD); Higgins (2003, 2004) (CFSGS) used Poisson's ratio equal to zero and Baker (1991) (CFSGS) reported that compared to D_x and D_y, the effect of D_1 is slight. Thus, Poisson's ratio can be assumed zero for convenience. Full details of the derivation of the above analytical solutions can be found in Turan (2009).

In order to demonstrate the effect of H on the deck performance, parametric studies using Eq. 5-10 were performed considering $H = \alpha\sqrt{D_x D_y}$ and varying the parameter α for each of the 3 cases of orthotropy described above. A 71.2 kN (16 kip) patch load with dimensions 254 mm x 508 mm (10 in. x 20 in.) was placed at the center of the span and using the analytical solutions, strong direction moment under the center of the patch versus α values were plotted in Fig. 3 for span lengths a= 1.52 m., 3.05 m., and 4.57 m. (5 ft, 10 ft, and 15 ft) and a range of orthotropic stiffness ratios, D=1, 2, 2.5, 5, 8, and 10, where $D = D_x / D_y$. It is observed that the moment values have large gradients for α between 0 and 1. However for α larger than 1, the gradients are not as large and application of Case 2 to decks that are torsionally stiff would provide conservative results. If the analytical solution for Case 2 ($\alpha = 1$) was applied to decks which are torsionally soft ($\alpha < 1$), the resulting moments would be unconservative. Thus, the current AASHTO-LRFD moment equations on section 4.6.2.1.8 require modification to allow for a unified treatment of decks of various types.

Current AASHTO-LRFD Live Load Moment Equations

The present AASHTO-LRFD (2007) provisions in section 4.6.2.1.8 define live load moment equations for two different cases: main bars transverse to traffic in N-mm/mm as:

$$M_{transverse_{(AASHTO)}}(L \leq 3000\ mm) = 1290 D^{0.197} L^{0.459} C \tag{11}$$

$$M_{transverse_{(AASHTO)}}(L > 3000\ mm) = \frac{5300 D^{0.188}(L^{1.35} - 20400)}{L} C \tag{12}$$

and main bars parallel to traffic in N-mm/mm as:

$$M_{parallel_{(AASHTO)}}(L \leq 3000\ mm) = 408 D^{0.123} L^{0.64} C \tag{13}$$

$$M_{parallel_{(AASHTO)}}(L > 3000\ mm) = \frac{3405 D^{0.138}(L^{1.429} - 34900)}{L} C \tag{14}$$

where C is the continuity factor (1.0 for simply supported and 0.8 for continues spans). These equations were derived based on $H = \sqrt{D_x D_y}$ and cannot capture the behavior of the decks when $H > \sqrt{D_x D_y}$ and $H < \sqrt{D_x D_y}$. Thus, to reflect other realistic stiffness characteristics of many different bridge deck types, they require modification as described in the previous section.

To develop similar design expressions considering all types of orthotropy, moving load analysis were done for arbitrarily placed patch loads across representative deck stiffness and span parameters. The two common design orientations of the main bars were investigated and the AASHTO-LRFD design notional live load models were considered in the present analyses. These include the design truck (AASHTO-LRFD 2007, section 3.6.1.2.2) and design tandem (AASHTO-LRFD 2007, section 3.6.1.2.3) live loads. . Unfactored truck patch loads were taken as 71.2 kN (16 kip) and tandem patch loads were taken as 55.6 kN (12.5 kip). The patch size was selected as a rectangle with dimensions of 254 mm x 508 mm (10 in. x 20 in) (AASHTO-LRFD 2007, section 3.6.1.2.5). The live load factor, γ, and dynamic load allowance percent, *IM*, were used as

1.75 and 33%, respectively, and directly implemented to the computed moment magnitudes. The main variables were selected as the span length, L from 0.91 m. (3 ft) to 6.10 m. (20 ft) with 0.31 m. (1 ft) increments; the stiffness ratio, D=1, 2, 2.5, 5, 8 and 10; and α = 0.25, 0.5, 0.75, 1, 2,4 and 8. Other than α, the main variables used in the current code are the same. However, to investigate the equations for use with open grid decks, span lengths less than 1.52 m. (5 ft), (the minimum span length used in Higgins (2003)) were also populated. In order to achieve adequate convergence, 30 terms were used to represent the infinite series solution for all analyses. The analysis results for the two common deck orientations are described and synthesized in the subsequent sections.

New Live Load Design Moment Equations for Main Bars Transverse to Traffic

For main bars transverse to the direction of traffic, two possible loading conditions, shown in Fig. 4, were used. Only one truck axle was used in the analyses as the other axle on the same truck is too far away (at least 4.27 m. (14 ft)) from the axle considered to produce an important change in the strong direction moment. Both axles of the tandem were considered as these are sufficiently close so as to jointly influence moment. Depending on the span length, either a single vehicle was placed on the deck with a multiple presence factor (MPF) of 1.2 or two vehicles were placed on the deck with an MPF of 1.0. For every D, and L value, the design truck and tandem patch loads were moved across the surface at 25.4 mm (1 in.) increments and the strong direction moments were calculated every 25.4 mm (1 in.) along the x-axis. Strong direction moments were multiplied with the corresponding MPF, IM, and γ and the maximum computed strong direction moments (M_{max_tr}) were recorded. Using M_{max_tr} data for the various deck spans, stiffness ratios, and α values (756 cases); two equations were obtained by nonlinear curve-fitting and rounding the fit parameters for design convenience to estimate the maximum strong direction moments in N-mm/mm as:

$$M_{transverse}(L \leq 3000\ mm) = \frac{1145 D^{0.214} L^{0.468}}{\alpha^{0.231}} C \tag{15}$$

$$M_{transverse}(L > 3000\ mm) = \frac{976 D^{0.194}(L^{1.55} - 99209)}{L\alpha^{0.233}} C \tag{16}$$

The form of these equations was selected to be similar to the current AASHTO-LRFD formulation but now include the influence of the relative torsional stiffness of the deck. These equations provide a direct method to capture the maximum strong direction moment produced in an orthotropic deck for design. The mean value for the ratio of M_{max_tr} to $M_{transverse}$ is 1.05 with maximum = 1.28, minimum = 0.91 and coefficient of variation = 0.07. M_{max_tr} versus $M_{transverse}$ are shown in Fig.5a and the equations provide a reasonable estimate of the maximum moments produced by the AASHTO notional design vehicles and offer a more unified framework for design of different deck types.

The proposed equations were also compared with AASHTO-LRFD (2007) section 4.6.2.1.8 equations (Eq 11-12) using α =1.0. Although the proposed equations and Eq. 11-12 should be identical when α =1.0, since different patch sizes (AASHTO 1994 and AASHTO-LRFD 2007 section 3.6.1.2.5) and additional points (D =5.0 and L =0.91 m., 1.22 m. (3ft, 4 ft)) were used in developing the present equations, results are slightly different as shown in Fig.5b. The mean value for the ratio of $M_{transverse}$ to $M_{transverse(AASHTO)}$ is 1.00 with maximum = 1.10, minimum = 0.94 and coefficient of variation = 0.04.

New Live Load Design Moment Equations for Main Bars Parallel to Traffic

For main bars parallel to the direction of traffic, two possible loading conditions, shown in Fig. 6, were used. Again, the second axle on the same truck is sufficiently far away from the considered axle such that the second truck axle was ignored. For any span length single or two vehicles were placed on the deck with MPF of 1.2 or 1.0. Since the MPF is 0.85 for three vehicles located on the deck, the strong direction moment contribution of the third vehicle is very small and ignored (Higgins 2003). Patch dimensions were changed according to the traffic direction and for every D, α and L value; design truck (single and two) and tandem (single and two) were marched across the deck at 25.4 mm (1 in.) increments. Strong direction moments were calculated along the x-axis at locations spaced 25.4 mm (1 in.) apart and multiplied with the corresponding MPF, IM, and γ. The maximum strong direction moments (M_{max_par}) were computed for the various spans, stiffness ratios, and relative torsional stiffnesses (756 cases). Nonlinear curve-fitting was performed on these data and the obtained fit coefficients rounded for design convenience to obtain the maximum strong direction moments for main bars oriented parallel to traffic as:

$$M_{parallel}(L \leq 3000\ mm) = \frac{581D^{0.12}L^{0.6}}{\alpha^{0.145}}C \tag{17}$$

$$M_{parallel}(L > 3000\ mm) = \frac{680D^{0.11}(L^{1.62} - 120461)}{L\alpha^{0.174}}C \tag{18}$$

These equations provide a mean value for the ratio of M_{max_par} to $M_{parallel}$ = 1.00 with maximum = 1.28, minimum = 0.90 and coefficient of variation = 0.06. The computed M_{max_tr} versus $M_{transverse}$ are shown in Fig.7a and as seen here, the equations provide a reasonable estimate of the maximum moments produced by the AASHTO notional design vehicles and framework for design.

The new equations were also compared with AASHTO-LRFD (2007) section 4.6.2.1.8 equations (Eq 13-14) using α = 1.0. Again, due to additional points and different patch size, the new equations are slightly different than Eq. 13-14 as seen in Fig.7b. The mean value for the ratio of $M_{parallel}$ to $M_{parallel(AASHTO)}$ is 1.04 with maximum = 1.11, min =0.99 and coefficient of variation =0.02.

Determination of Rigidities for Decks

In order to use the proposed formulas (Eq. 15-18); D_x, D_y, and α are needed. AASHTO-LRFD (2007) states that D_x and D_y can be calculated using transformed area method as the moment of inertia times the modulus of elasticity for a unit width of deck. Cracked section properties should be considered in the calculation. Experimentally, for the strong direction flexural rigidity, the deck can be simply supported at the edges and a line load can be applied at the center, parallel to the supports, as shown in Fig 8a. In order to better visualize the loading conditions, the deflected shape of a steel grid deck partially filled with concrete from a finite element model are shown in Fig. 8. Since this load does not produce curvature in the orthogonal direction, the deck can be analyzed as a beam and the flexural stiffness of the beam (or unit width of the deck) can be calculated using the deflection and the applied load. The same procedure can be followed for weak direction stiffness as shown in Fig 8b.

For α , since Poisson's ratios in the x and y direction were set to zero, which sets D_1 zero; $H = 2D_{xy} = \alpha\sqrt{D_x D_y}$. To establish α , D_x , D_y , and D_{xy} are needed. The D_x and D_y stiffnesses are determined as above and D_{xy} is determined experimentally according to Tsai (1965). Here the plate is loaded at the corner, shown in Fig. 8c, and using the center deflection or the corner deflection under the load, D_{xy} and α can be calculated as:

$$D_{xy} = \frac{PL^2}{4w_L} \text{ or } D_{xy} = \frac{PL^2}{16w_o} \tag{19}$$

where P , w_L and w_o are point load applied at the corner, deflection under the point load and the deflection at the center of the plate, respectively. The resulting α values can be computed as:

$$\alpha = \frac{PL^2}{2\sqrt{D_x D_y}\, w_L} \text{ or } \alpha = \frac{PL^2}{8\sqrt{D_x D_y}\, w_o} \tag{20}$$

For decks, the D_{xy} stiffness values should be determined in the uncracked range as field observations of decks do not tend to exhibit torsional cracking that would result at large twisting loads.

Conclusion

The current AASHTO-LRFD Specification uses many different design provisions to establish live load design demands in bridge decks with approximately 17% of Chapter 4 used to prescribe analysis of decks. To unify analysis methods for establishing live load moments in decks, a generalized approach was developed. The approach uses a general orthotropic plate model that considers all of the cases of orthotropy: 1) relatively torsionally stiff, flexurally soft decks; 2) relatively uniformly thick deck (such as a reinforced concrete deck); and 3) relatively torsionally soft, flexurally stiff decks. Using orthotropic plate theory, analytical expressions were derived for calculating strong direction moments under arbitrary patch loading. The expressions were used in concert with the AASHTO-LRFD notional live load models to sweep all possible patch load locations across a deck surface to establish design maxima for two common deck orientations: main bars oriented transverse to the direction of traffic and main bars oriented parallel to the direction of traffic. From thousands of moving load analysis results, semi-analytical expressions were fit to the analysis results considering a range of practical stiffness ratios, span lengths, and relative torsional stiffness values. The AASHTO-LRFD prescribed impact, multiple presence, and live load factors were incorporated into the solutions to establish Strength I design live load moment magnitude. Using the proposed formulations, bridge deck strength design demands can now be treated in a unified way across different deck types using only four equations. Experimental methods were also presented that can be used to empirically establish the elastic rigidities for use in the design equations. Application of these methods can significantly reduce and greatly simplify analysis of decks and allow bridge engineers to better compare different deck design alternatives.

REFERENCES

American Association of State Highway and Transportation Officials (AASHTO-LRFD), (2004). *LRFD Bridge Design Specifications*, 3rd Edition, Washington, D.C.

American Association of State Highway and Transportation Officials (AASHTO-LRFD), (2007). *LRFD Bridge Design Specifications*, 4th Edition, Washington, D.C.

American Association of State Highway and Transportation Officials (AASHTO-LRFD), (1994). *LRFD Bridge Design Specifications*, 1st Edition & Interims, Washington, D.C.

Baker, T. H. (1991). "Plate Stiffness Constants for Concrete Filled Steel Grid Decks.: Static and Fatigue Strength Determination of Design Properties for Grid Decks," Vol. I, Research Report St-9, Dept of Civil Eng., U. of Pittsburg, Pittsburg, PA.

Gangarao, H. V. S., Raju, P. R., and Koppula N. R. (1992). "Behavior of Concrete-Filled Steel Grid Decks." *Transportation Research Record*, 1371, Transportation Research Board, Washington, D.C., 1-7.

Higgins, C., (2003). "LRFD Orhtotropic Plate Model for Live Load Moment in Filled Grid Decks." *ASCE, Journal of Bridge Engineering*, Vol. 8, No. 1, 20-28.

Higgins, C. (2004). "Orthotropic Plate Model for Estimating Deflections in Filled Grid Decks." *ASCE Journal of Bridge Engineering*, 9(6), 599-605.

Huang, H. Chajes, M. J., Mertz, D. R., Shenton, H. W., and Kaliakin, V. N. (2002) "Behavior of Open Steel Grid Decks for Bridges." *Journal of Constructional Steel Research*, v 58, n 5-8, 819-842.

Huang, H., Kaliakin, V. N., Chajes, M. J., Mertz, D. R., and Shenton, H. W. (2007). "Application of Orthotropic Thin Plate Theory to Filled Steel Grid Decks for Bridges." *ASCE Journal of Bridge Engineering*, 12 (6), 807-810.

Mangelsdorf, C. P., Baker, T. H., and Swanson, J. A. (2002). "Predicting Deflections in Concrete-Filled Grid Deck Panels." *Transportation Research Record*, 1814, Transportation Research Board, Washington, D.C., 17-24.

Turan O. T. (2009) "Design, Analysis and Evaluation of Bridge Superstructures for Live Loads" PhD Thesis, Oregon State University, Corvallis, OR.

Tsai S. W. (1965) "Experimental Determination of the Elastic Behavior of Orthotropic Plates" *ASME Journal of Engineering for Industry*, 315-317.

Figures:

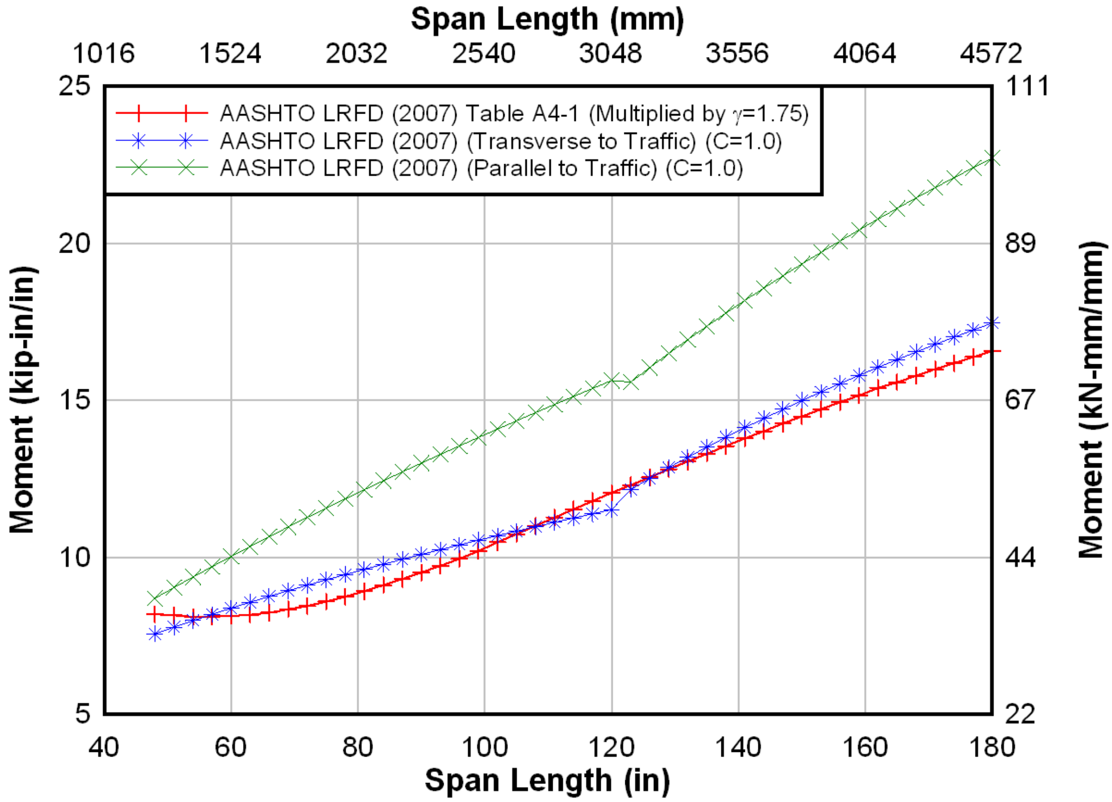

Fig 1. AASHTO-LRFD (2007) moment values for D=1.0 and C=1.0, and AASHTO-LRFD (2007) deck slab design table positive moment values.

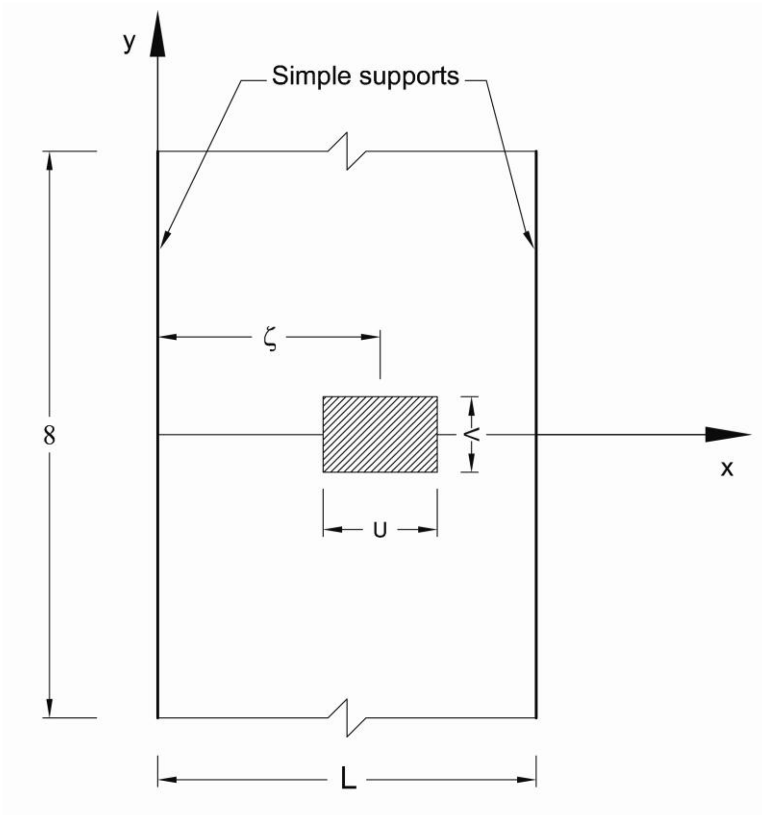

Fig. 2. Uniformly loaded single patch load located on an infinitely wide and simply supported orthotropic plate

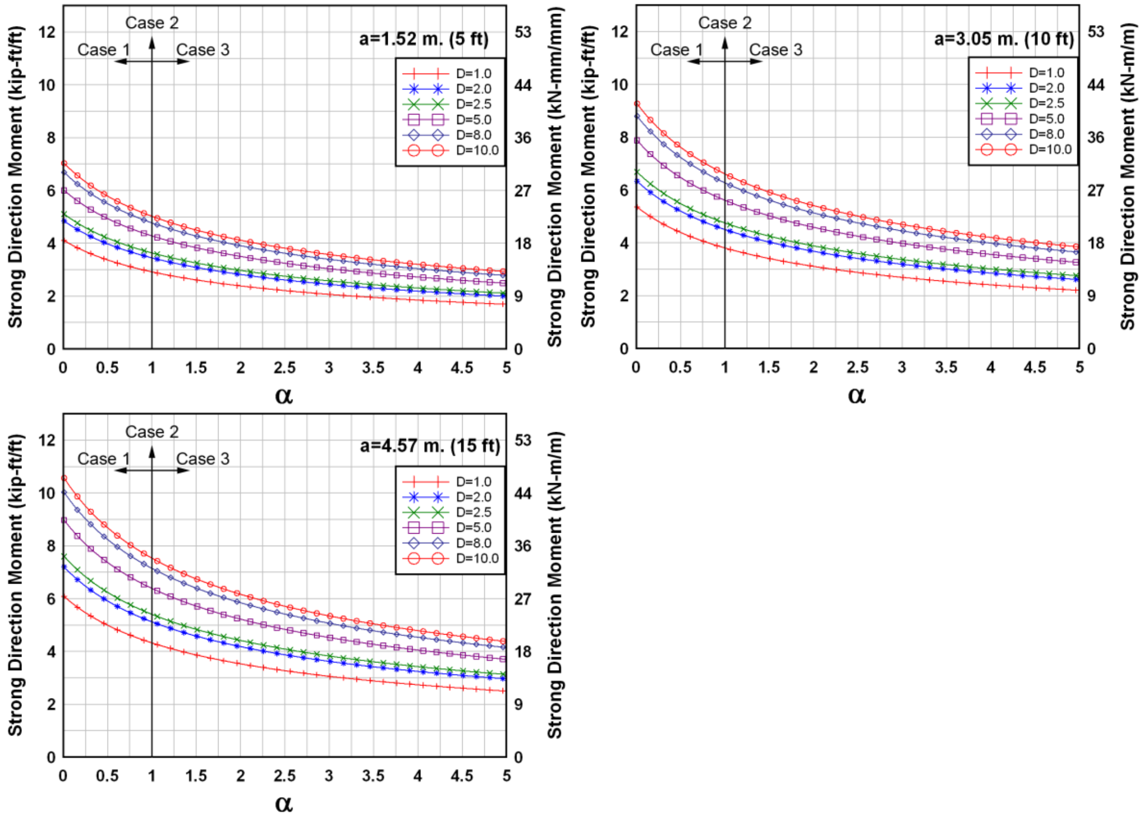

Fig. 3. Strong direction moment under the center of the patch versus α values.

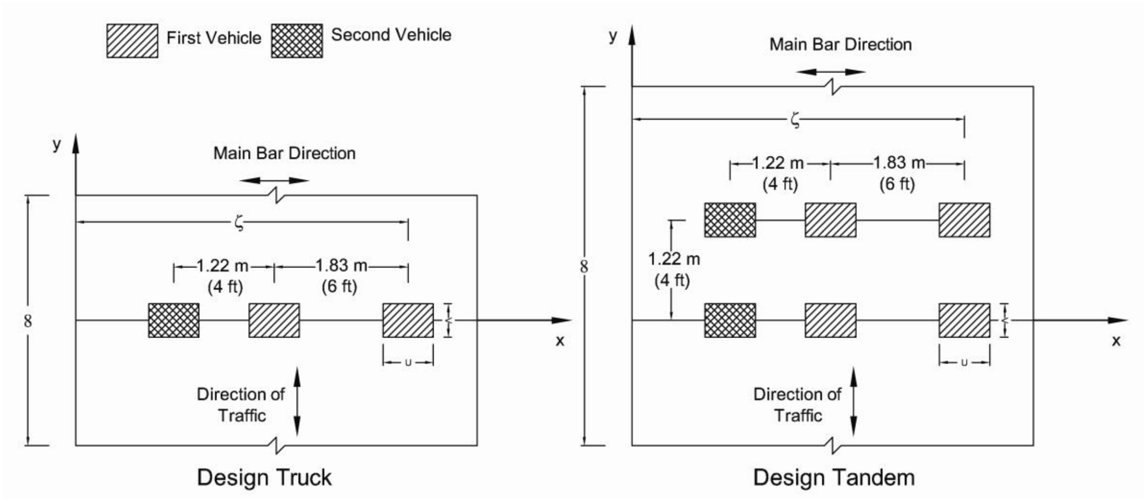

Fig. 4. Design truck and design tandem loads for main bars transverse to direction of traffic.

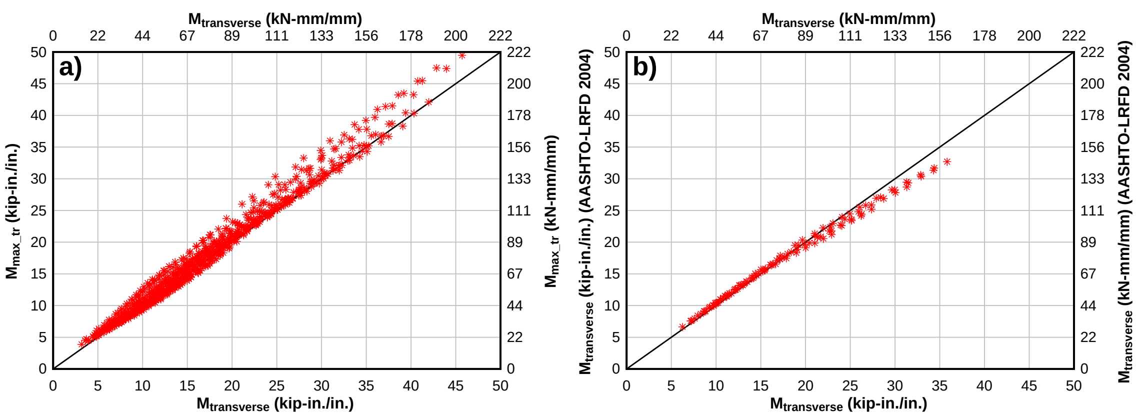

Fig. 5. a) M_{max_tr} versus $M_{transverse}$ b) $M_{transverse(AASHTO)}$versus $M_{transverse}$

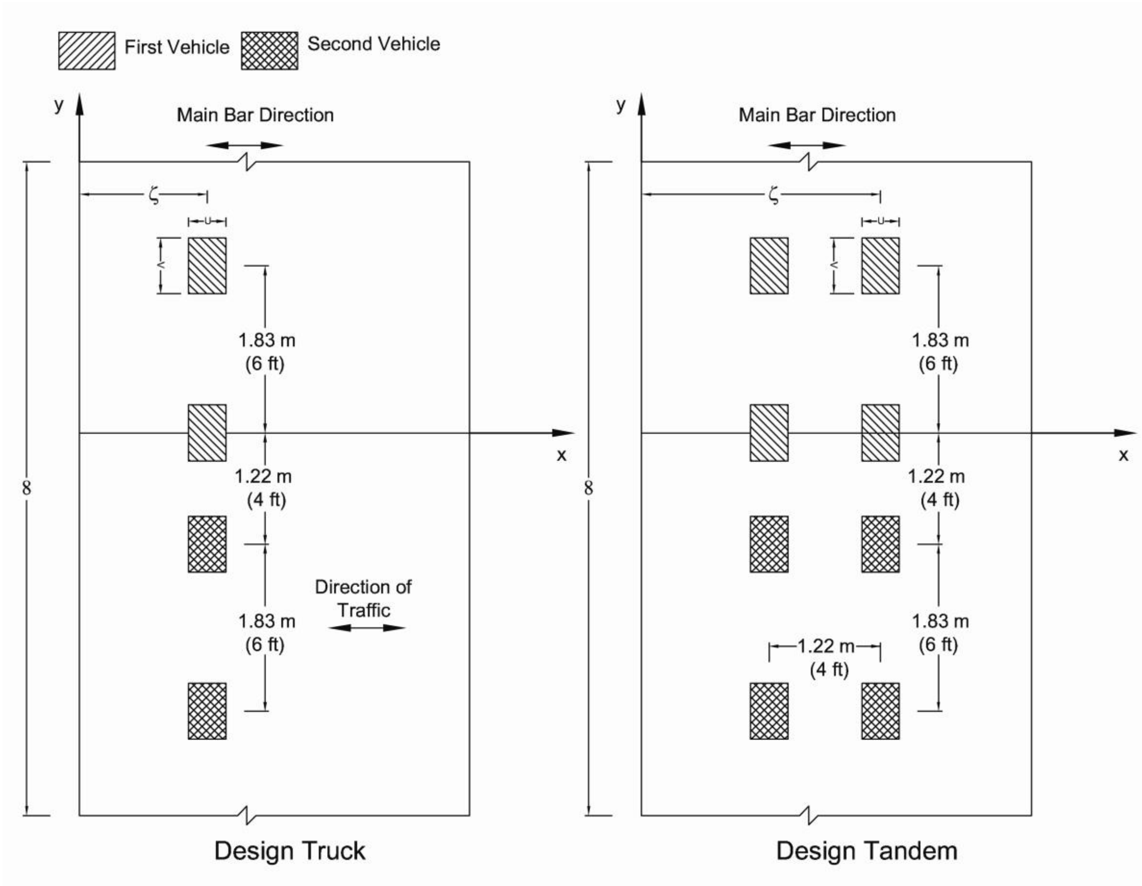

Fig. 6. Design truck and design tandem loads for main bars parallel to direction of traffic.

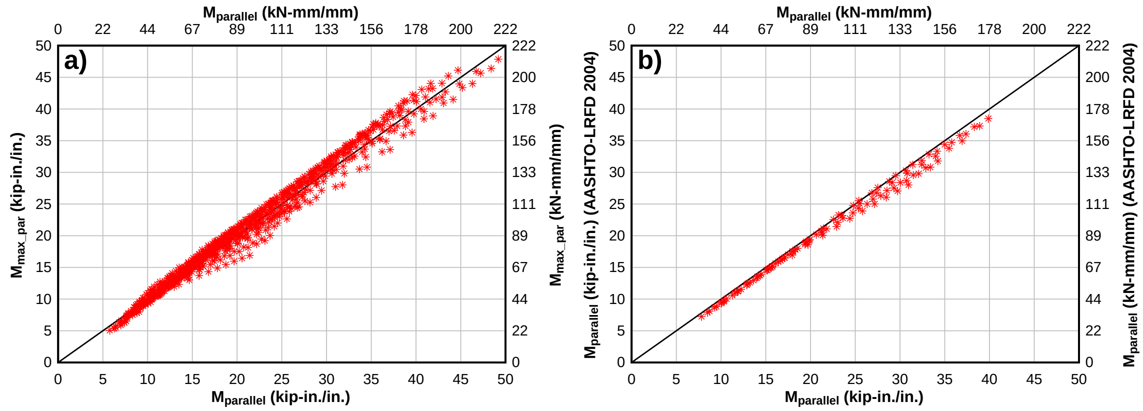

Fig. 7. a) M_{max_par} versus $M_{parallel}$ b) $M_{parallel(AASHTO)}$versus $M_{parallel}$

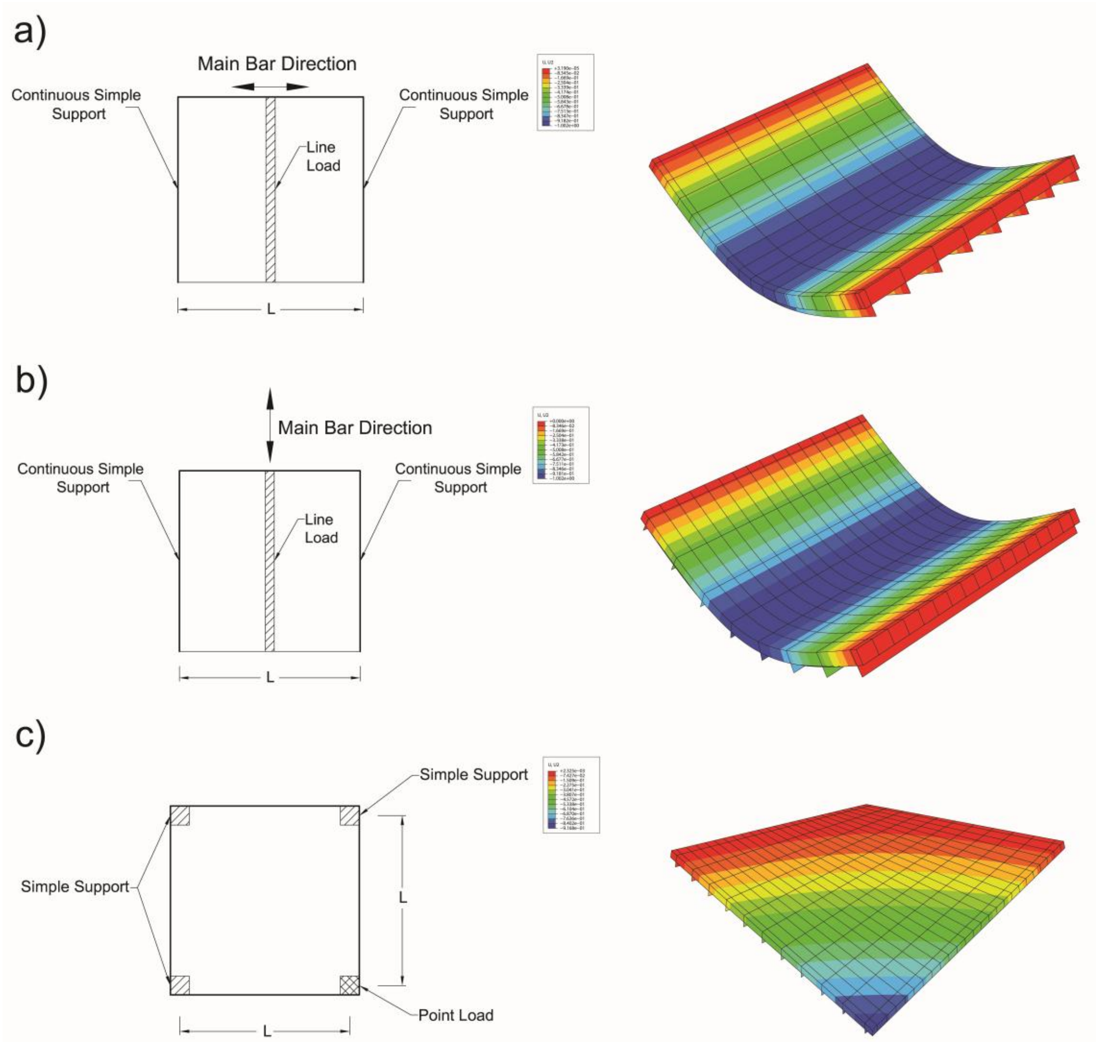

Fig. 8. a) Main bars transverse to supports (D_x) b) Main bars parallel to supports (D_y) c) Twist test (D_{xy})